Feature Extraction based on Vector Hydrophone in the Waveguide Environment

Lanyue ZHANG[1], Xiaoying YAO[2],Desen YANG[3]

[1,2,3]*College of Underwater Acoustic Engineering, Harbin Engineering University, Harbin 150001*

Email：[1]zhanglanyue@hrbeu.edu.cn

Abstract: Unlike in the free field, the propagation characteristics of acoustic waves in the waveguide are influenced by the boundary surface. And with the application of vector hydrophone, particle velocity has been widely used in some areas of underwater acoustic signal processing. In this paper, first, in contrast with the free filed, the features of sound pressure and particle velocity of the noise radiated from the target in the waveguide were extracted separately using the time-domain theory and the frequency domain theory. And then two kinds of experimental data were studied, and the scalar and vector features were obtained. The research results showed that the laws of acoustic propagation in the waveguide were more complicated than that in the free field. And more information of sound field of targets was obtained using vector hydrophone than using pressure hydrophone and the distinguishing probability could be improved.

Key Word: Vector hydrophone, Waveguide, Feature Extract.

1. Introduction

The ocean development has become a heat issue in the current world, and the marine research attracts more and more attention recently. Compared with the deep sea, the shallow sea is closely connected to the human's life [1]. Therefore, it is especially important to study the propagation characteristics of acoustic waves in the shallow water. With the development of the vector hydrophone, some achievements [2]-[3] have been obtained in the modeling with the vector sound field and feature extraction from the vector information, but, the characteristics of the noise of the target in the waveguide need to be more studied using the combination of the modeling with the vector sound field and feature extraction from the vector information. Based on the above all, in this paper, the scalar and vector characteristics from the noise of target in the waveguide and free field were analyzed, and the scalar and vector features were obtained through different feature extraction methods.

2. Data models of the ship-radiated noise

The underwater target radiation noise is composed of hydrodynamic noise, mechanical noise and propeller noise, which is characterized by continuous broadband spectrum and line-component spectrum. Because the frequency stability and uniqueness of the line spectrum, which takes the parameters of the target type and motion, it has significance for the target detection and recognition to study the features of the line spectrum. This paper mainly discussed the line spectrum.

2.1 Data models of the ship-radiated noise in free field

Free field is an ideal environment. Therefore, it has great theoretic implications to study the propagating characters of sound waves in the free field. The propeller discrete noise is main part of the vessel noise, and the line spectrum which is always harmonics is produced. The relation between the m th harmonic and the blade frequency was mathematically stated as:

$$f_m = mB\,\frac{s}{60} \tag{1}$$

Where B and s were number of blade and speed of propeller respectively.

The mathematics model of acoustic vector signal was expressed as:

This work was supported by major Programs of china(Grant No.6121221-01 and Grant No.51303020307-4)

$$\begin{cases} p(t) = \sum_m A_m \cos(2\pi f_m t) + n_p(t) \\ v_r(t) = \cos(\theta) \cdot \sum_m \frac{A_m}{\rho c} \cos(2\pi f_m t) + n_{vr}(t) \\ v_z(t) = \sin(\theta) \cdot \sum_m \frac{A_m}{\rho c} \cos(2\pi f_m t) + n_{vz}(t) \end{cases} \quad (2)$$

Where A_m represented the amplitude of the corresponding line spectrum and θ denoted the angle between incident direction and the horizontal surface.

Next, we presented the simulation waveform of the acoustic vector signal. The specification of the bearing was as follows: sampling frequency,10240Hz; speed of propeller,1800r/min;number of the blade, 6; number of the line spectrum, 10; distance between the hydrophone and sound source,1000m. Noise is gauss noise, whose frequency bandwidth was same as the signal. The results were exemplified in Fig.1.

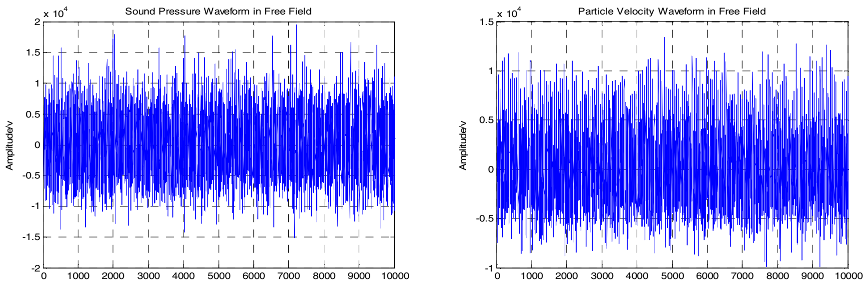

a.Sound pressure waveform b. Particle velocity waveform

Fig.1. Time-domain waveform in free field

2.2 Data models of the ship-radiated noise in waveguide

In waveguide, the effect of the boundary surface on the acoustics waves should be considered. In this article, the sea surface and the sea floor were seen as horizontal plane and the virtual source method [4] was used to simulate the signal. The principle of the virtual source method was shown in Fig.2:

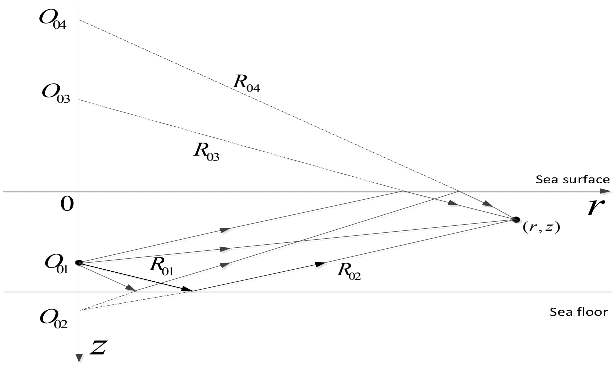

Fig.2. The principle of the virtual source method

Based on the principle of linear superposition, the sound pressure in the receiving points was the sum of the pressure of the real source and all virtual sources. So, the sound pressure was modeled as:

$$p(t,r,z) = p(t)\sum_{l=0}^{\infty}\left[(VV_{l1})^l \frac{e^{jkR_{l1}}}{R_{l1}} + (VV_{l2})^l V_{l2} \frac{e^{jkR_{l2}}}{R_{l2}} + (VV_{l3})^l V \frac{e^{jkR_{k3}}}{R_{l3}} + (VV_{l4})^{l+1} \frac{e^{jkR_{l4}}}{R_{l4}}\right] \quad (3)$$

Here, k was wave number; r signified the horizontal distance between the sound source and hydrophone; $R_{li} = (r^2 + Z_{li}^2)^{1/2}$ represented distance between the receiving point and the virtual source which corresponding to the i th sound ray of the l th rank virtual source, i=1~4 indicated four sound rays for each rank virtual source: For example, when l=0, Z_{01} was the direct sound ray, Z_{02} was the sound ray reflected once by the sea beds, Z_{03} was the sound ray reflected once by the sea surface, Z_{04} was the sound ray which was reflected by the sea beds first and then by the sea surface; V denoted the reflection coefficient of the sea surface, which was a constant; V_{li} represented the reflection coefficient of the sea beds for the i th sound ray of the l th rank virtual source, which was expressed as:

$$V_{li} = \frac{m\cos\theta_{li} - \sqrt{n^2 - \sin^2\theta_{li}}}{m\cos\theta_{li} + \sqrt{n^2 - \sin^2\theta_{li}}} \tag{4}$$

Where m was density ratio of sea water to seabed medium, and n was ratio of the sound speed in sea water to that in seafloor.

According to the Euler equation: $\rho \cdot \mathrm{d}\boldsymbol{v}/\mathrm{d}t = -\nabla p$, where ρ was the density of sea water. Using the following equation:

$$\frac{\partial V_{li}}{\partial r} = \frac{\partial V_{li}}{\partial \theta}\cdot\frac{\partial \theta}{\partial r} = \frac{z_{li}}{R_{li}^{2}}\frac{\partial V_{li}}{\partial \theta}, \quad \frac{\partial V_{li}}{\partial z} = \frac{\partial V_{li}}{\partial \theta}\cdot\frac{\partial \theta}{\partial z} = \frac{r}{R_{li}^{2}}\frac{\partial V_{li}}{\partial \theta}$$

The horizontal and vertical particle velocity were wrote as:

$$\begin{aligned} v_r = \frac{p(t)}{\mathrm{j}\omega\rho}\sum_{l=0}^{\infty}\Bigg[& lV^{l}V_{l1}^{l-1}\frac{\mathrm{d}V_{l1}}{\mathrm{d}\theta_{l1}}\frac{z_{l1}}{R_{l1}^{3}}\mathrm{e}^{\mathrm{j}kR_{l1}} + (VV_{l1})^{l}\frac{r(\mathrm{j}kR_{l1}-1)}{R_{l1}^{3}}\mathrm{e}^{\mathrm{j}kR_{l1}} + (l+1)V^{l}V_{l2}^{l}\frac{\mathrm{d}V_{l2}}{\mathrm{d}\theta_{l2}}\frac{z_{l2}}{R_{l2}^{3}} \\ & \cdot\mathrm{e}^{\mathrm{j}kR_{l2}} + (VV_{l2})^{l}V_{l2}\frac{r(\mathrm{j}kR_{l2}-1)}{R_{l2}^{3}}\mathrm{e}^{\mathrm{j}kR_{l2}} + lV^{l+1}V_{l3}^{l-1}\frac{\mathrm{d}V_{l3}}{\mathrm{d}\theta_{l3}}\frac{z_{l3}}{R_{l3}^{3}}\mathrm{e}^{\mathrm{j}kR_{l3}} + (VV_{l3})^{l}V \\ & \cdot\frac{r(\mathrm{j}kR_{l3}-1)}{R_{l3}^{3}}\mathrm{e}^{\mathrm{j}kR_{l3}} + (l+1)V^{l+1}V_{l4}^{l}\frac{\mathrm{d}V_{l4}}{\mathrm{d}\theta_{l4}}\frac{z_{l4}}{R_{l4}^{3}}\mathrm{e}^{\mathrm{j}kR_{l4}} + (VV_{l4})^{l+1}\frac{r(\mathrm{j}kR_{l4}-1)}{R_{l4}^{3}}\mathrm{e}^{\mathrm{j}kR_{l4}}\Bigg] \end{aligned}$$

$$\begin{aligned} v_z = \frac{p(t)}{\mathrm{j}\omega\rho}\sum_{l=0}^{\infty}\Bigg[& lV^{l}V_{l1}^{l-1}\frac{\mathrm{d}V_{l1}}{\mathrm{d}\theta_{l1}}\frac{-r}{R_{l1}^{3}}\mathrm{e}^{\mathrm{j}kR_{l1}} + (VV_{l1})^{l}\frac{z_{l1}(\mathrm{j}kR_{l1}-1)}{R_{l1}^{3}}\mathrm{e}^{\mathrm{j}kR_{l1}} + (l+1)V^{l}V_{l2}^{l}\frac{\mathrm{d}V_{l2}}{\mathrm{d}\theta_{l2}} \\ & \cdot\frac{-r}{R_{l2}^{3}}\mathrm{e}^{\mathrm{j}kR_{l2}} + (VV_{2})^{l}V_{l2}\frac{z_{l2}(\mathrm{j}kR_{l2}-1)}{R_{l2}^{3}}\mathrm{e}^{\mathrm{j}kR_{l2}} + lV^{l+1}V_{l3}^{l-1}\frac{\mathrm{d}V_{l3}}{\mathrm{d}\theta_{l3}}\frac{-r}{R_{l3}^{3}}\mathrm{e}^{\mathrm{j}kR_{l3}} + (VV_{l3})^{l}V \\ & \cdot\frac{z_{l3}(\mathrm{j}kR_{l3}-1)}{R_{l3}^{3}}\mathrm{e}^{\mathrm{j}kR_{l3}} + (l+1)V^{l+1}V_{l4}^{l}\frac{\mathrm{d}V_{l4}}{\mathrm{d}\theta_{l4}}\frac{-r}{R_{l4}^{3}}\mathrm{e}^{\mathrm{j}kR_{l4}} + (VV_{l4})^{l+1}\frac{z_{l4}(\mathrm{j}kR_{l4}-1)}{R_{l4}^{3}}\mathrm{e}^{\mathrm{j}kR_{l4}}\Bigg] \end{aligned}$$

Where θ_{li} denoted the incident angle of the i th sound ray of the l th rank virtual source.

We assumed values for the parameters as shown in the table.1 to simulate the signal in the waveguide.

parameters	values	parameters	values
Sea-water density/kg•m^{-3}	1000	Source depth/m	35
Sea-floor density/kg•m^{-3}	1800	Receiver depth/m	25
Sound velocity in sea-water/m•s^{-1}	1500	Water depth/m	50
Sound velocity in sea-floor/ m•s^{-1}	1613	Horizontal distance/m	1000

Table.1 Parameters for the model of waveguide

The results of the simulation were depicted in Fig.3:

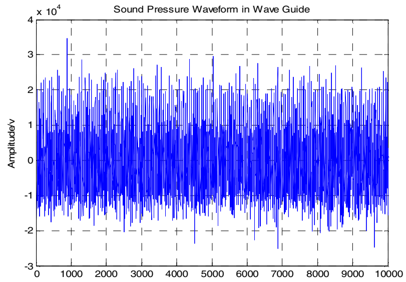

a.Sound pressure waveform

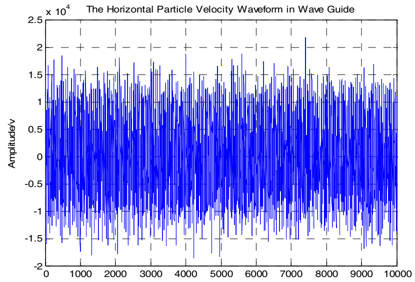

b.Horizontal particle velocity waveform

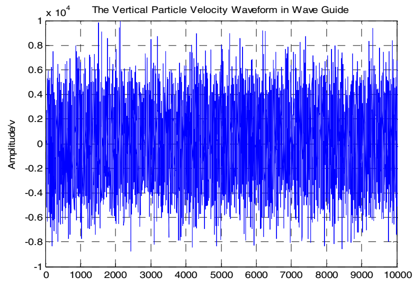

c. Vertical particle velocity waveform

Fig.3. Time-domain waveform in waveguide

3. Features extraction methods

During feature extraction, mathematic description of the physical property of signal radiated from the target was made firstly; and then, with the help of various transformations, the essential characteristics of the target were obtained. At present, according to the domains, feature extraction methods can be divided into four groups: time-domain, frequency domain, time-frequency domain and transform domain. In this paper, the time domain and frequency domain methods were used to extract features from underwater signal.

3.1 Time domain method

Peak to peak amplitude, zeros crossing points (ZCP) and wave area are common time domain method. Clear principle and concise physical meaning made ZCP become a fine method to process the underwater signal.

The number of ZCP [5] was defined as the number of the intersection point of signal waveform and horizontal (time) axis, which was related to the spectrum of signal. When the spectrum changed, the number of ZCP would change. With the low-frequency signal, the number of ZCP was smaller. On the contrary, it was larger with the high-frequency signal. Due to these properties, ZCP was appropriate to analyze the ship-radiated noise.

The ZCP of the simulation data in section 2 were shown in the following figures:

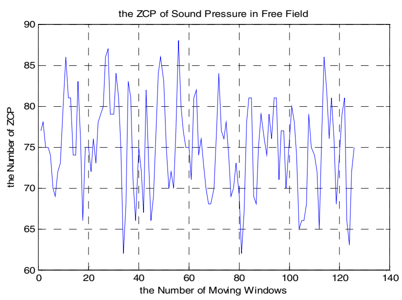

a.The ZCP of sound pressure

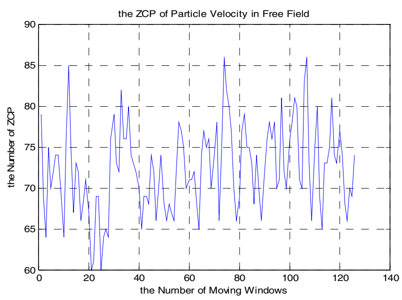

b.The ZCP of particle velocity

Fig.4 The ZCP of the simulation data in free field

As depicted in Fig.4, there was obvious difference between the ZCP of sound pressure and that of particle velocity. The average values were 75.5 and 72.3 respectively, which illustrated that the spectrum of sound pressure and that of particle velocity had a little difference in free field. And the variance of particle velocity was smaller than that of the pressure that means particle velocity was steadier than sound pressure.

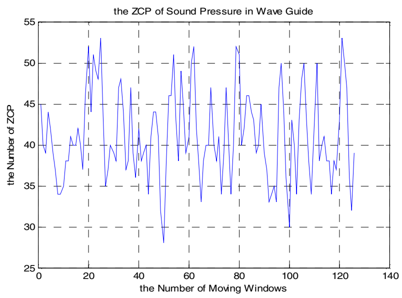

a.The ZCP of sound pressure

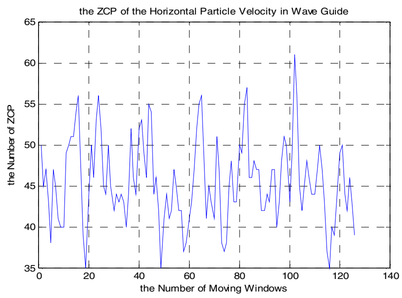

b.The ZCP of horizontal particle velocity

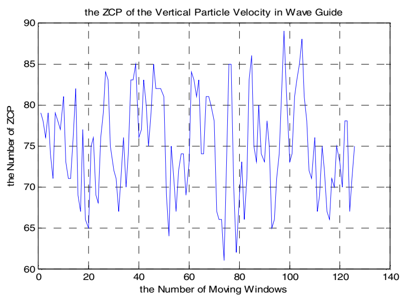

c. The ZCP of vertical particle velocity

Fig.5. The ZCP of the simulation data in wave guide

Compared with the free field in Fig.4, significant changes happened in the ZCP of the simulation data in waveguide illustrated in Fig.5. The mean value of the ZCP of sound pressure was 41.14, and the variance became 29.37, that means, duo to the reflection of the boundary surface, the ZCP of sound pressure became much steadier. As for the ZCP of horizontal and vertical particle velocity, the average values were 45.65 and 75.07 and the variances were 26.48 and 37.38 respectively, which meant there was some similarity, which was different from the ZCP of vertical particle velocity, in the ZCP of sound pressure and that of horizontal particle velocity.

3.2 Frequency domain method

Frequency domain analysis is the most common and basic signal process method, which apply various transform to obtain frequency feature of signal. Frequency domain method was an efficient technique to analyze the ship-radiated noise which has obvious characteristic of line spectrum. In the paper, we dealt with the data with power spectrum estimation.

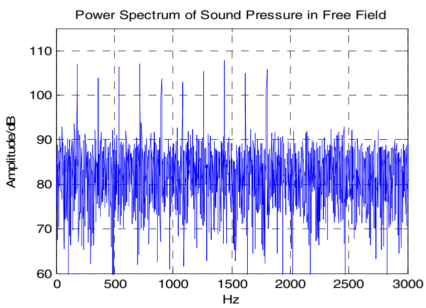

a.Power spectrum of sound pressure

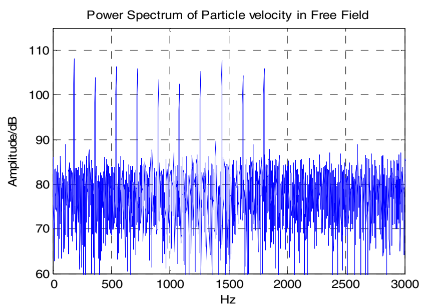

b.Power spectrum of particle velocity

Fig.6. Power spectrum of the simulation data in free field

Fig.6 indicated the difference between the power spectrum of sound pressure and that of particle velocity in free field. Compared with sound pressure, particle velocity was less influenced by noise.

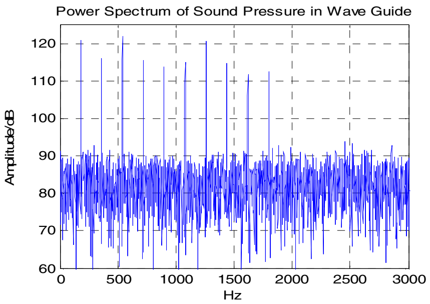

a.Power spectrum of sound pressure

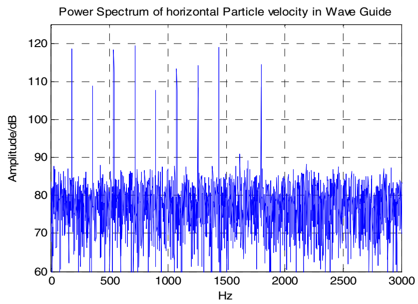

b.Power spectrum of horizontal particle velocity

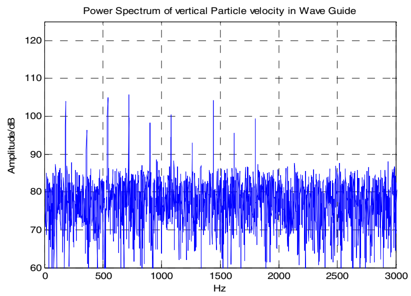

b.Power spectrum of vertical particle velocity

Fig.7. Power spectrum of the synthetic data in waveguide

Due to the effect of sea surface and seafloor, the attenuation of the power of sound wave was smaller and the power at the receiver point was much bigger than that in free field. As given in Fig.7(a), the amplitude of line spectrum of sound pressure was bigger than that in free field. Because of the different effect on the scalar and vector information in waveguide, the results of the particle velocity was very different from sound pressure. In Fig.7(b), the power spectrum of the horizontal velocity was similar to that of sound pressure expect the noise sensitivity and rare line spectrum. And in Fig.7(c), the result of vertical particle velocity was obvious different from others which corresponding to the difference of the ZCP distribution in section 3.1.

4. Experienced data analysis

In this paper, two kinds of ship-radiated noise were analyzed. The sampling frequencies were 3152Hz and 4096Hz respectively. The length of window was 320 when the ZCP was extracted from data. The results were depicted in the following figures.

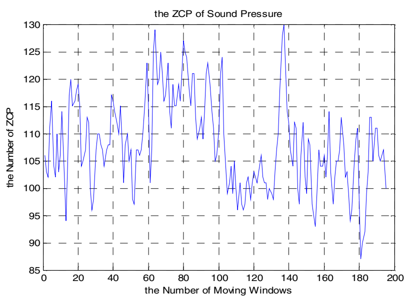

a.The ZCP of sound pressure

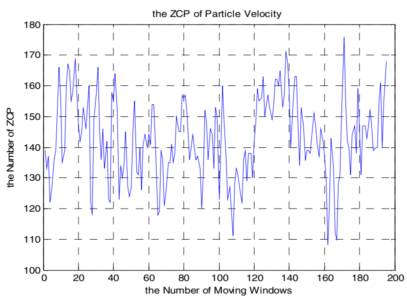

b.The ZCP of particle velocity

Fig.8. The ZCP of the first kind of real data

Fig.8 showed that there was big difference between sound pressure and particle velocity of the same kind of experienced data. The variance of sound pressure was smaller than that of particle velocity, which meant the ZCP of pressure was much steadier.

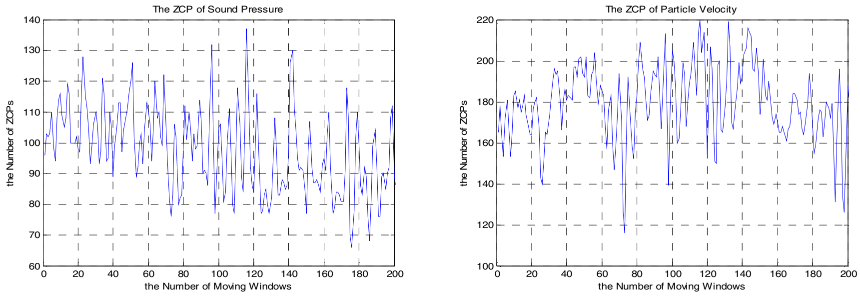

a.The ZCP of sound pressure b.The ZCP of particle velocity

Fig.9. The ZCP of the second kind of real data

The ZCP of the second kind of experienced data illustrated in Fig.9 was compared to that of the first kind depicted in Fig.8, there was obvious difference between them. And in Fig.9, the ZCP of sound pressure and particle vibrating velocity were also very different, so the ZCP of ship-radiated noise can be used to do target discrimination.

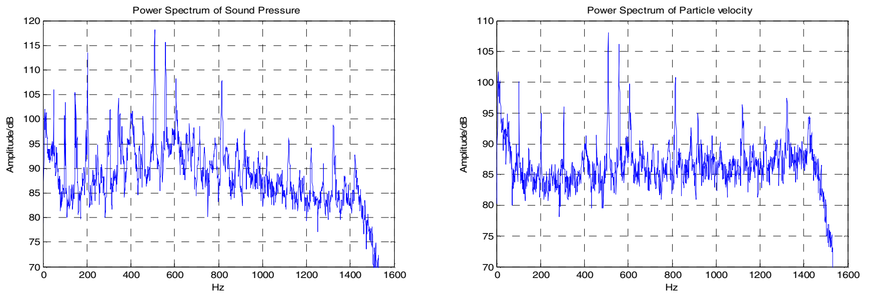

a.Power spectrum of sound pressure b.Power spectrum of particle velocity

Fig.10 Power spectrum of the first kind of real data

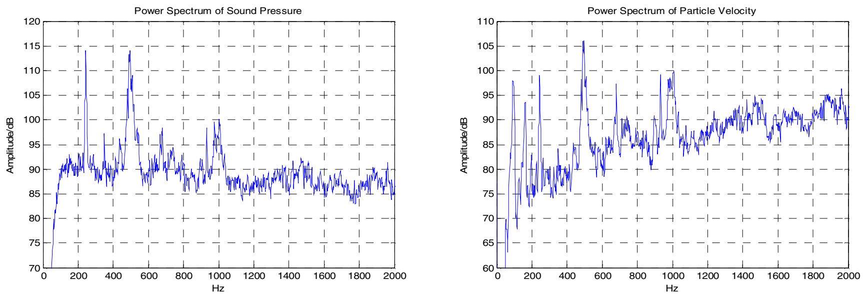

a.Power spectrum of sound pressure b.Power spectrum of particle velocity

Fig.11 Power spectrum of the second kind of real data

Compared Fig.11with Fig.10, the power spectrum of the two kinds of real data had obvious difference. So the power spectrum of target-radiated noise also can be used to do target discrimination. And for each kind of the experienced data, the power spectrum of sound pressure was significant different from that of particle velocity. For the first kind of target, sound pressure contained more line spectrum information, but for the second kind of target, particle velocity contained more information.

5. Target identification

In this section, we used BP neural network [6] with one hidden layer to distinguish two kinds of experienced data which were analyzed in section 4. There were 100 samples for each kind of data, with 50 samples as training set and the others as the test set. The results of identification were shown in table 2:

Kind of target Feature extraction	The first kind of target		The second kind of target	
	Sound pressure	Particle velocity	Sound pressure	Particle velocity
Time-domain method	74%	78%	86%	84%
Frequency-domain method	88%	94%	86%	100%

Table.2 The results of identification

As shown in the table.2, the identification probability of particle velocity was higher than that of sound pressure. And compared with the time-domain feature, the identification probability of the frequency-domain feature was higher.

6. Conclusion

In this paper, we analyzed the ship-radiated noise in waveguide with the time-domain method and frequency-domain method, we found the signal was much more complicated than that in free field. The boundary surface of the waveguide made different effects which were needed to be further researched on sound pressure and particle velocity, and the identification probability of the target discrimination using the particle velocity was higher than that using sound pressure.

Reference:

[1] B G Katsnelson and V G Petnikpv. *Shallow water acoustics*. Springer Praxis publishing.2002.

[2] Li Sichun, Yang Desen, Lu Yang. Extraction of line Spectra and Azimuth Distinguish about Two Targets by Single Vector Hydrophone.*Proceedings of the 4th International Symposium on Acoustic Engineering and Technology.Beijing：National Defense Industy Press*, pp. 52-255, 2006.

[3] Melvin J.Hinich, Davide Marandino and Edmund J.Sullivan.Bespectrum of ship-radiated noise. J.Acoust.Soc.Am, pp. 1512-1517, 1998.

[4] JI．M．Brekhovskikh． *Foundamentals of Ocean Acoustics*.New York: Springer Verlag.1985

[5] Zhou You, Han Peng and Xiang Jinglin. Analysis and Application of Ship-radiated Noise's Zero-crossing Number.*Journal of Detection & Control*. pp. 64-67, 2007.

[6] L Bruzzone. Structured neural networks for signal classification. *Signal Processing*. pp. 271-290, 1998.